2008 IEEE/RSJ International Conference on Intelligent Robots and Systems
Acropolis Convention Center
Nice, France, Sept, 22-26, 2008

A Pattern Generator of Humanoid Robots Walking on a Rough Terrain using a Handrail

Ken'ichi Koyanagi and Hirohisa Hirukawa
University of Tsukuba and AIST
1-1-1 Tenohdai, Tsukuba, 305-8571 Japan
hiro.hirukawa@aist.go.jp

Shizuko Hattori, Mitsuharu Morisawa, Shin'ichiro Nakaoka
Kensuke Harada and Shuuji Kajita
National Institute of Advanced Industrial Science and Technology
1-1-1 Umezono, Tsukuba 305-8568 Japan

***Abstract*— This paper presents a biped humanoid robot that is able to walk on a rough terrain while touching a handrail. The contact wrench sum (CWS for short) is used as the criterion to judge if the contact between the robot and the environment is strongly stable under the sufficient friction assumption, where the contact points are not coplanar and the normal vectors at the points are not identical. It is confirmed that the proposed pattern generator can make the robot walk as desired in dynamics simulations and experiments, and the motions can be improved by a hand position control and using waist joints.**

I. INTRODUCTION

The ZMP (Zero Moment Point)[15] has been used as a stability criterion to judge if the contact between a foot of a legged robot and a floor should be kept while walking. It can judge the strong stability of a contact, where a contact is called strongly stable if it is guaranteed that the contact should be kept to a given external wrench[13]. A number of walking pattern generators have been proposed using the ZMP as the strong stability criterion (See [12], [11], [6] for example). But the ZMP is a rigorous stability criterion only when the contact points between the robot and the environment are coplanar and the normal vectors at the points are identical under the sufficient friction assumption.

When the ZMP is used to plan motion patterns of a robot that walks on a terrain other than a flat plane and/or a contact between a hand and the environment, some approximations should be introduced to judge the contact stability. For example, Harada et al. proposed a generalized ZMP[2] that can judge the contact stability under an approximation assumption, and presented a humanoid robot that can go up the stairs while catching a handrail [3].

Recently it was proved that the contact should be strongly stable if the contact wrench sum (CWS for short) is an internal element of the contact wrench cone (CWC for short) when the contact points are neither coplanar and the normal vectors at the points nor identical under the sufficient friction assumption, and that the CWS and CWC are equivalent to the ZMP and the supporting polygon respectively when the robot walks on a flat plane without a hand contact[4]. The CWS was used to generate walking patterns of a biped humanoid robot that walks on a rough terrain[5]. This paper uses the CWS as the contact stability criterion to generate motion patterns of a biped humanoid robot that walks on a rough terrain while touching a handrail. The motion patterns are examined on dynamics simulator OpenHRP3[16], [10] and successufully applied to control a real humanoid robot with a hand position modification.

This paper is organized as follows. Section 2 outlines the motion pattern generator based on the CWS. Section 3 presents how a humanoid robot can walk on a rough terrain with a support of a handrail. Section 4 concludes the paper.

II. PATTERN GENERATOR

A. Equations of Momentum

Let $p_B, \boldsymbol{v}_B, \boldsymbol{\omega}_B$ be the position, velocity and the angular velocity of the coordinates on the waist link of a humanoid robot respectively which is supposed to have six degrees of the freedom in the space with respect to the reference coordinates. Let n be the number of the joints connected to the link and $\dot{\boldsymbol{\theta}} : n \times 1$ the angular velocity of the joints. See Fig.1. Then the momentum of the robot $\mathcal{P}$ and the angular momentum about the center of the gravity $\mathcal{L}$ can be given by

$$\begin{bmatrix} \mathcal{P} \\ \mathcal{L} \end{bmatrix} = \begin{bmatrix} M\boldsymbol{E} & -M\hat{\boldsymbol{r}}_{B\to G} & \boldsymbol{M}_{\dot{\theta}} \\ \boldsymbol{0} & \tilde{\boldsymbol{I}} & \boldsymbol{H}_{\dot{\theta}} \end{bmatrix} \begin{bmatrix} \boldsymbol{v}_B \\ \boldsymbol{\omega}_B \\ \dot{\boldsymbol{\theta}} \end{bmatrix}, \quad (1)$$

where M is the total mass of the robot, $\boldsymbol{E}$ the 3×3 unit matrix, $\boldsymbol{r}_{B\to G}$ the position vector from the origin of the waist coordinates to the COG of the robot, $\tilde{\boldsymbol{I}} : 3 \times 3$ the inertia matrix about the COG, $\boldsymbol{M}_{\dot{\theta}} : 3 \times n$, $\boldsymbol{H}_{\dot{\theta}} : 3 \times n$ the inertia matrices which relate the joint velocities into the momentum and the angular momentum of the robot respectively. $\hat{}$ is the operator converting a 3×1 vector into a 3×3 skew-symmetric matrix whose multiplication from the left makes a vector product. Let x, y, z axes of the waist coordinates point to the front, left and top respectively.

Eq.(1) transforms $n+6$ velocity variables into 6 momentum variables, but in general the degrees of the freedom of the robot should degenerate because of the contact between the robot and the working environment. Let $\boldsymbol{v}_{F_i}, \boldsymbol{\omega}_{F_i}$ be the velocity and the angular velocity of the coordinates fixed at the i-th foot link ($i = 1, 2$), and $\boldsymbol{v}_{H_i}, \boldsymbol{\omega}_{H_i}$ those of the coordinates at the i-th hand link ($i = 1, 2$) respectively. $\boldsymbol{v}_{F_i}, \boldsymbol{\omega}_{F_i}$ and $\boldsymbol{v}_{H_i}, \boldsymbol{\omega}_{H_i}$ are constrained by the contact or by reference trajectories, and Eq.(1) under the constraints can

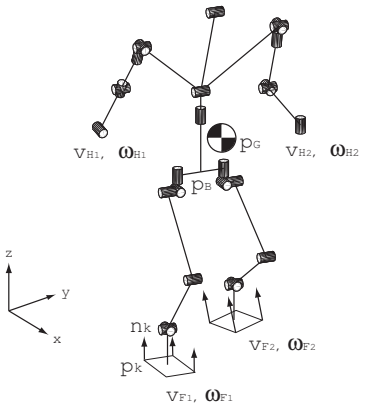

Fig. 1. Definitions of the coordinates

be given by

$$\begin{bmatrix} \mathcal{P} \\ \mathcal{L} \end{bmatrix} = \begin{bmatrix} \boldsymbol{M}_B^* \\ \boldsymbol{H}_B^* \end{bmatrix} \boldsymbol{\xi}_B + \sum_{i=1}^{2} \{ \begin{bmatrix} \boldsymbol{M}_{F_i}^* \\ \boldsymbol{H}_{F_i}^* \end{bmatrix} \boldsymbol{\xi}_{F_i} + \begin{bmatrix} \boldsymbol{M}_{H_i}^* \\ \boldsymbol{H}_{H_i}^* \end{bmatrix} \boldsymbol{\xi}_{H_i} \}, \tag{2}$$

where

$$\boldsymbol{\xi}_B \equiv \begin{bmatrix} \boldsymbol{v}_B \\ \boldsymbol{\omega}_B \end{bmatrix}, \quad \boldsymbol{\xi}_{F_i} \equiv \begin{bmatrix} \boldsymbol{v}_{F_i} \\ \boldsymbol{\omega}_{F_i} \end{bmatrix}, \quad \boldsymbol{\xi}_{H_i} \equiv \begin{bmatrix} \boldsymbol{v}_{H_i} \\ \boldsymbol{\omega}_{H_i} \end{bmatrix},$$

and $\boldsymbol{M}_B^*$, $\boldsymbol{H}_B^*$, $\boldsymbol{M}_{F_i}^*$, $\boldsymbol{H}_{F_i}^*$, $\boldsymbol{M}_{H_i}^*$, and $\boldsymbol{H}_{H_i}^*$ are the inertia matrices under the constraints and given by

$$\begin{aligned} \begin{bmatrix} \boldsymbol{M}_B^* \\ \boldsymbol{H}_B^* \end{bmatrix} &\equiv \begin{bmatrix} M\boldsymbol{E} & -M\hat{\boldsymbol{r}}_{B\to G} \\ \boldsymbol{0} & \tilde{\boldsymbol{I}} \end{bmatrix} \\ &\quad - \sum_{i=1}^{2} \begin{bmatrix} \boldsymbol{M}_{F_i}^* \\ \boldsymbol{H}_{F_i}^* \end{bmatrix} \begin{bmatrix} \boldsymbol{E} & -\hat{\boldsymbol{r}}_{B\to F_i} \\ \boldsymbol{0} & \boldsymbol{E} \end{bmatrix} \\ &\quad - \sum_{i=1}^{2} \begin{bmatrix} \boldsymbol{M}_{H_i}^* \\ \boldsymbol{H}_{H_i}^* \end{bmatrix} \begin{bmatrix} \boldsymbol{E} & -\hat{\boldsymbol{r}}_{B\to H_i} \\ \boldsymbol{0} & \boldsymbol{E} \end{bmatrix}, \\ \begin{bmatrix} \boldsymbol{M}_{F_i}^* \\ \boldsymbol{H}_{F_i}^* \end{bmatrix} &\equiv \begin{bmatrix} \boldsymbol{M}_{leg_i} \\ \boldsymbol{H}_{leg_i} \end{bmatrix} \boldsymbol{J}_{leg_i}^{-1}, \\ \begin{bmatrix} \boldsymbol{M}_{H_i}^* \\ \boldsymbol{H}_{H_i}^* \end{bmatrix} &\equiv \begin{bmatrix} \boldsymbol{M}_{arm_i} \\ \boldsymbol{H}_{arm_i} \end{bmatrix} \boldsymbol{J}_{arm_i}^{-1}, \end{aligned}$$

where $\boldsymbol{J}_{leg_i}, \boldsymbol{J}_{arm_i}$ are 6×6 Jacobian matrices determined by the kinematics of the legs and arms, $\boldsymbol{r}_{B\to F_i}$ the position vector from the origin of the waist coordinates to the i-th foot coordinates, $\dot{\boldsymbol{\theta}}_{leg_i} (i = 1, 2)$ and $\dot{\boldsymbol{\theta}}_{arm_i} (i = 1, 2)$ 6×1 joint velocity vectors of the legs and the arms respectively, and the inertia matrices are decomposed into

$$\begin{aligned} \dot{\boldsymbol{\theta}} &= [\dot{\boldsymbol{\theta}}_{leg_1}^T \quad \dot{\boldsymbol{\theta}}_{leg_2}^T \quad \dot{\boldsymbol{\theta}}_{arm_1}^T \quad \dot{\boldsymbol{\theta}}_{arm_2}^T]^T, \\ \boldsymbol{M}_{\dot{\theta}} &= [\boldsymbol{M}_{leg_1} \ \boldsymbol{M}_{leg_2} \ \boldsymbol{M}_{arm_1} \ \boldsymbol{M}_{arm_2}], \\ \boldsymbol{H}_{\dot{\theta}} &= [\boldsymbol{H}_{leg_1} \ \boldsymbol{H}_{leg_2} \ \boldsymbol{H}_{arm_1} \ \boldsymbol{H}_{arm_2}], \end{aligned}$$

whose components correspond to two legs and two arms respectively [7]. Note that the inverse of the Jacobian can be replaced by the pseudo-inverse when a leg or an arm has more than 6 DOF.

Since the reference of $\boldsymbol{v}_{F_i}, \boldsymbol{\omega}_{F_i}$ and $\boldsymbol{v}_{H_i}, \boldsymbol{\omega}_{H_i}$ are given, the joint velocity of the legs and the arms can be given by

$$\dot{\boldsymbol{\theta}}_{leg_i} = \boldsymbol{J}_{leg_i}^{-1} \begin{bmatrix} \boldsymbol{v}_{F_i} \\ \boldsymbol{\omega}_{F_i} \end{bmatrix} - \boldsymbol{J}_{leg_i}^{-1} \begin{bmatrix} \boldsymbol{E} & -\hat{\boldsymbol{r}}_{B\to F_i} \\ \boldsymbol{0} & \boldsymbol{E} \end{bmatrix} \begin{bmatrix} \boldsymbol{v}_B \\ \boldsymbol{\omega}_B \end{bmatrix}, \tag{3}$$

$$\dot{\boldsymbol{\theta}}_{arm_i} = \boldsymbol{J}_{arm_i}^{-1} \begin{bmatrix} \boldsymbol{v}_{H_i} \\ \boldsymbol{\omega}_{H_i} \end{bmatrix} - \boldsymbol{J}_{arm_i}^{-1} \begin{bmatrix} \boldsymbol{E} & -\hat{\boldsymbol{r}}_{B\to H_i} \\ \boldsymbol{0} & \boldsymbol{E} \end{bmatrix} \begin{bmatrix} \boldsymbol{v}_B \\ \boldsymbol{\omega}_B \end{bmatrix}, \tag{4}$$

from the reference of $(\boldsymbol{v}_B, \boldsymbol{\omega}_B)$, and then the reference of the angular momentum $\mathcal{L}^{ref}$ is found by Eq.(1).

B. Equations of the Contact Wrench

Let the sum of the gravity and the inertia force applied to the robot be $\boldsymbol{f}_G$ and the sum of the moments about the COG of the robot $\boldsymbol{\tau}_G$ with respect to the reference coordinates, which can be given by

$$\boldsymbol{f}_G = M(\boldsymbol{g} - \ddot{\boldsymbol{p}}_G), \tag{5}$$

$$\boldsymbol{\tau}_G = \boldsymbol{p}_G \times M(\boldsymbol{g} - \ddot{\boldsymbol{p}}_G) - \dot{\mathcal{L}}, \tag{6}$$

where $\boldsymbol{p}_G$ is the position vector of the COG with respect to the reference coordinates and $\boldsymbol{g} = [0 \ 0 \ -g]^T$ the gravity vector. Let us assume that sufficient friction exists at the contact. The assumption implies that an arbitrary friction force can be generated at every contact point with a positive normal force. Then the set of the contact wrench can be written by

$$\boldsymbol{f}_C = \sum_{k=1}^{K} \epsilon_k (\boldsymbol{n}_k + \sum_{l=1}^{2} \delta_k^l \boldsymbol{t}_k^l), \tag{7}$$

$$\boldsymbol{\tau}_C = \sum_{k=1}^{K} \boldsymbol{p}_k \times \epsilon_k (\boldsymbol{n}_k + \sum_{l=1}^{2} \delta_k^l \boldsymbol{t}_k^l), \tag{8}$$

where $\boldsymbol{n}_k$ is the unit normal vector at the k-th contact point $\boldsymbol{p}_k$, $\boldsymbol{t}_k^l (l = 1, 2)$ the unit tangent vectors at $\boldsymbol{p}_k$ whose linear combination spans the tangent plane at $\boldsymbol{p}_k$, ϵ_k a non-negative scalar, δ_k^l a scalar, and K the number of the contact points. See Fig.1 again. Let us call the set of the contact wrench *Contact Wrench Cone* or *CWC* for short, since the set forms a polyhedral convex cone. Then the strong contact stability can be determined as follows[4].

Theorem 1: **(Strong stability criterion)** If $(-\boldsymbol{f}_G, -\boldsymbol{\tau}_G)$ is an internal element of the CWC given by Eqs.(7) and (8), then the contact is strongly stable to $(\boldsymbol{f}_G, \boldsymbol{\tau}_G)$ [4].

When $(-\boldsymbol{f}_G, -\boldsymbol{\tau}_G)$ is an internal element of the CWC, $(\boldsymbol{f}_G, \boldsymbol{\tau}_G)$ should balance with the sum of the contact wrench. We call the sum the *Contact Wrench Sum* or *CWS* for short. The pattern generator plans the reference trajectory of the CWS, and then find the reference trajectory of the COG by solving the equations of the contact wrench which can be derived by balancing the right hand sides of Eqs.(5) and (6) and those of Eqs.(7) and (8) respectively[4].

Let $\boldsymbol{p}_G = (x_G, y_G, z_G)$, $\boldsymbol{p}_k = (x_k, y_k, z_k)$, $\mathcal{L} = (\mathcal{L}_x, \mathcal{L}_y, \mathcal{L}_z)$, $\boldsymbol{n}_k = (n_{kx}, n_{ky}, n_{kz})$ and $\boldsymbol{t}_k^l = (t_{kx}^l, t_{ky}^l, t_{kz}^l)$. The reference of the COG is planned based on the equations of the contact wrench as follows. At first, let us plan the

reference of $\ddot{z}_G$. Then the force along the z-axis should balance as

$$M(\ddot{z}_G + g) = \sum_{k=1}^{K} \epsilon_k n_{kz} + \sum_{k=1}^{K} \epsilon_k \sum_{l=1}^{2} \delta_k^l t_{kz}^l, \quad (9)$$

in which the ratio between the first and second terms of the right hand side is arbitrary and we choose it as

$$\sum_{k=1}^{K} \epsilon_k n_{kz} = (1-\alpha) M(\ddot{z}_G + g), \quad (10)$$

$$\sum_{k=1}^{K} \epsilon_k \sum_{l=1}^{2} \delta_k^l t_{kz}^l = \alpha M(\ddot{z}_G + g), \quad (11)$$

where $0 \leq \alpha < 1$ is a ratio to distribute the vertical force to friction, but has no rigorous physical meaning.

Next ϵ_k should be chosen so that $0 < \epsilon_k$ holds for at least three k to keep the strong stability of Theorem 1. For example, the reference of ϵ_k can be chosen to be

$$\epsilon_k^{ref} = (1-\alpha) M(\ddot{z}_G + g) \frac{\lambda_k^{ref}}{\sum_{k=1}^{K} \lambda_k^{ref} n_{kz}}, \quad (12)$$

by using $0 < \lambda_k^{ref} \leq 1$ for three k at least. When the robot touches a handrail at $\boldsymbol{p}_k$, λ_k has to be chosen to make the normal force at $\boldsymbol{p}_k$ large enough for supporting the body and small enough for preventing the hand from breaking. But there is no reasonable criterion to determine λ_k. We found a reasonable value of λ_k by dynamic simulations.

Then the reference trajectories of x_G, y_G are planned to follow the equations of the moments about the x and y axes

$$M(\ddot{z}_G + g)(y_G - y_C) - M\ddot{y}_G(z_G - z_C) + \dot{\mathcal{L}}_x = \sum_{k=1}^{K} \epsilon_k (y_k n_{kz} - z_k n_{ky}) \equiv \tau'_{Cx}, \quad (13)$$

$$-M(\ddot{z}_G + g)(x_G - x_C) + M\ddot{x}_G(z_G - z_C) + \dot{\mathcal{L}}_y = -\sum_{k=1}^{K} \epsilon_k (x_k n_{kz} - z_k n_{kx}) \equiv \tau'_{Cy}, \quad (14)$$

where y_C, z_C, x_C are defined by

$$y_C = \alpha \textstyle\sum_{k=1}^{K} \frac{\epsilon_k}{\epsilon} y_k, \quad z_C = (1-\alpha) \sum_{k=1}^{K} \frac{\epsilon_k}{\epsilon} z_k, \quad (15)$$

$$x_C = \alpha \textstyle\sum_{k=1}^{K} \frac{\epsilon_k}{\epsilon} x_k, \quad \epsilon = \sum_{k=1}^{K} \epsilon_k, \quad (16)$$

and $\tau'_{Cx(y)}$ is the moment about $x(y)$-axis excluding that from the friction force. It is guaranteed that the robot can be stopped finally, when the trajectory of the CWS is planned to have zero velocity at the end and the differential equations (13) and (14) are solved to satisfy the boundary condition.

C. Resolved Momentum Control

Let the solution of the equations of Eqs.(13) and (14) be (x_G^{ref}, y_G^{ref}), the reference of the momentum $(\mathcal{P}_x^{ref}, \mathcal{P}_y^{ref}, \mathcal{P}_z^{ref})$ can be given by

$$\mathcal{P}_x^{ref} = M\dot{x}_G^{ref}, \quad (17)$$

$$\mathcal{P}_y^{ref} = M\dot{y}_G^{ref}, \quad (18)$$

$$\mathcal{P}_z^{ref} = M\dot{z}_G^{ref}. \quad (19)$$

From Eq.(2), the reference of ξ_B can be found by the resolved momentum control[7] as

$$\boldsymbol{\xi}_B = \boldsymbol{A}^{-1}\boldsymbol{y}, \quad (20)$$

where

$$\boldsymbol{y} \equiv \begin{bmatrix} \mathcal{P}^{ref} \\ \mathcal{L}^{ref} \end{bmatrix} - \sum_{i=1}^{2} \begin{bmatrix} \boldsymbol{M}_{F_i}^* \\ \boldsymbol{H}_{F_i}^* \end{bmatrix} \boldsymbol{\xi}_{F_i}^{ref} - \sum_{i=1}^{2} \begin{bmatrix} \boldsymbol{M}_{H_i}^* \\ \boldsymbol{H}_{H_i}^* \end{bmatrix} \boldsymbol{\xi}_{H_i}^{ref},$$

$$\boldsymbol{A} \equiv \begin{bmatrix} \boldsymbol{M}_B^* \\ \boldsymbol{H}_B^* \end{bmatrix}.$$

Finally, the joint velocity of the robot can be obtained by Eqs.(3) and (4).

III. WALKING USING A HANDRAIL

A. Reference of the CWS

Let us consider the example shown in Fig.2, in which the robot is supposed to walk to the positive x direction and the handrail is set along the same axis. When the right hand

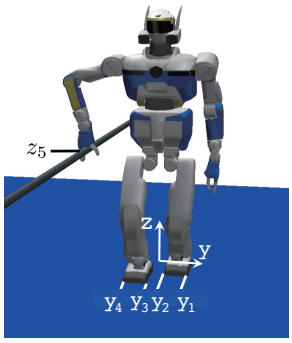

Fig. 2. Example of a humanoid robot touching a handrail

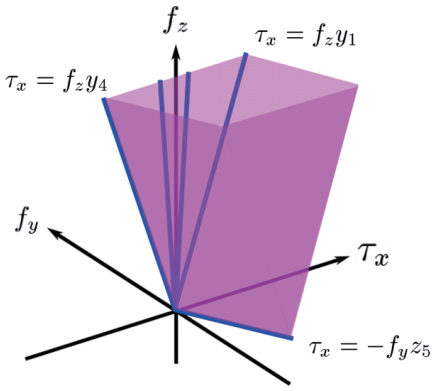

Fig. 3. Example of the CWC when the robot touches the handrail

of the robot touches the handrail, the hand can have a force from the handrail.

Let y coordinate of the lateral sides of the left and right feet be y_1, y_2, y_3 and y_4 respectively, and z of the contact point between the right hand and the handrail be z_5. Then the CWC in $f_y f_z \tau_x$-space formed by the normal forces from the lateral sides of the feet and the contact point of the hand can

be given in Fig.3. When the robot does not touch the handrail, the CWC is reduced to that on $f_z\tau_x$-plane. It is observed that the strongly stable region of the CWS is extended by introducing the half line $\tau_x = -f_y z_5$ corresponding to the normal force at the hand. Note that the force to the negative y can give a larger region than that to the positive z in the case.

It is guaranteed theoretically that the contact between the robot and the environment consisting of the handrail and the floor should be stable if the CWS is an internal element of the CWC. The claim is equivalent to the statement that the contact between the robot and the floor should be stable if the ZMP is an internal element of the CWC when the robot walks on a flat floor. The reference CWS has to be determined to let the normal force at the hand, ϵ_k in Eq.(12), stay between the minimum to support the body robustly and the maximum to prevent the hand from breaking. When humanoid robot HRP-2[9] is used as the target robot, the maximum of ϵ_k at the contact point of the hand is set to 100[N] considering the mechanical property of the robot. Note that the reference CWS can be planned from the forces at the contact points but it is not possible to control a force at a specific contact point due to the indetermination of the contact forces. Fig.4 shows several walking patterns of the robot while changing the reference CWS. The ratio of the normal force at the hand is smallest in the left picture and is largest in the right one.

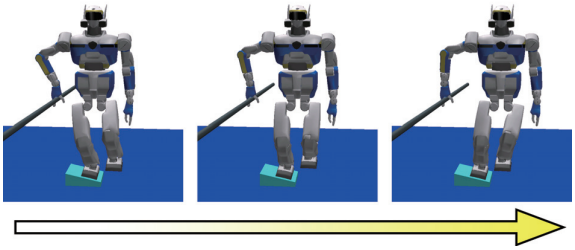

Fig. 4. Motion patterns depending on the normal force at the hand

Let us condsider an example in which humanoid robot HRP-2 walks over two boxes whose top faces are tilted about x-axis to two sides by 0.2 [rad] respectively. Then the pattern generator can plan the walking motion shown in Fig.5, where the motion is examined by dynamics simulator OpenHRP3, and the corresponding experiment is shown in Fig.6. The robot steps over the first box and has to stop then, because the reachable range of the hand is limited and therefore the hand is not able to touch the first and the second contact points from any intermediate position. The problem will be fixed in a later section.

The hand tries to touch the handrail rather than grasping it, since the reachable range of the hand should be smaller when it grasps an object. The outputs from the force sensor at the wrist of the right hand in the simulation (left) and the experiment (right) are shown respectively in Fig.7, where the hand touches at the first contact point of the handrail in the middle of the graphs. It is observed that the hand

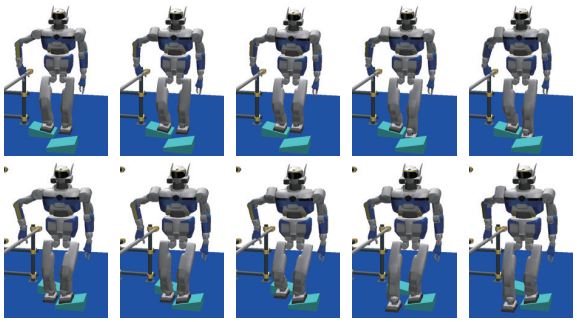

Fig. 5. Walking over tilted boxes (dynamics simulation)

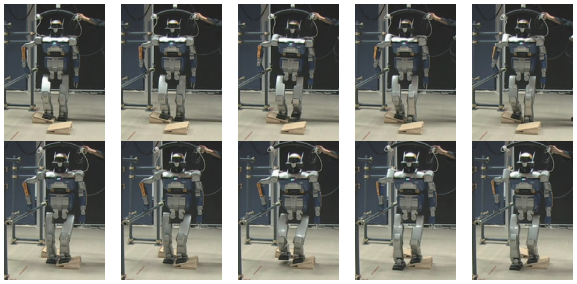

Fig. 6. Walking over tilted boxes (experiment)

has the force to the negative y direction as desired, which corresponds to the motion illustrated in Fig.2, and that the simulation result should coincide with the experimental one sufficiently. The trajectories of the CWS in the simulation and the experiment are shown respectively in Fig.8, where the CWC is drawn with $\delta_k^l = 0.5, \forall k, l$, because the sufficient friction assumption may not be hold in the physical world. The real CWS moves around the reference one mainly due to the spring and dumper mechanism at the feet of HRP-2 and the feedback control to stabilize the CWS.

B. Hand position control

Generally a feedback control is applied to stabilize the walking motions, then the $\boldsymbol{v}_B, \boldsymbol{\omega_B}$ may have a disturbance $\Delta\boldsymbol{v}_B, \Delta\boldsymbol{\omega_B}$ and the position of the hand should change from the reference trajectory which may let the hand leave from

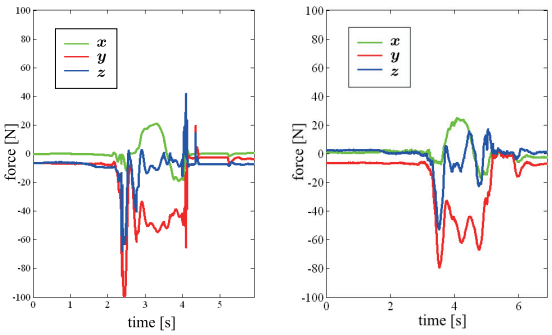

Fig. 7. Force sensor outputs in the simulation and the experiment

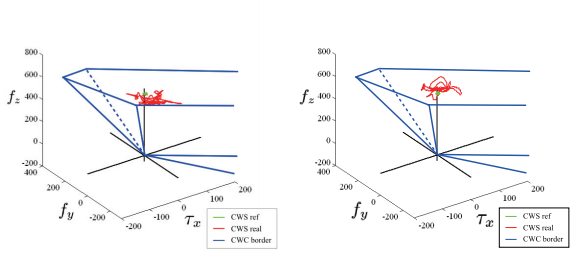

Fig. 8. Trajectories of the CWS in the simulation and the experiment

the handrail. When the feedback control is applied to change the joint angles of the legs, we can know $\Delta \boldsymbol{v}_B, \Delta \boldsymbol{\omega}_B$ from the forward kinematics of the legs and Eq.(4) can be modified into

$$\dot{\boldsymbol{\theta}}_{arm_i} = \boldsymbol{J}_{arm_i}^{-1} \left(\begin{bmatrix} \boldsymbol{v}_{H_i} \\ \boldsymbol{\omega}_{H_i} \end{bmatrix} - \begin{bmatrix} \boldsymbol{E} & -\hat{\boldsymbol{r}}_{B\to H_i} \\ \boldsymbol{0} & \boldsymbol{E} \end{bmatrix} \begin{bmatrix} \boldsymbol{v}'_B \\ \boldsymbol{\omega}'_B \end{bmatrix} \right),$$

where $\boldsymbol{v}'_B = \boldsymbol{v}_B + \Delta \boldsymbol{v}_B$, $\boldsymbol{\omega}'_B = \boldsymbol{\omega}_B + \Delta \boldsymbol{v}_B$ and the position of the hand can follow the reference trajectory. The pictures in the first row of Fig.9 show the hand and the handrail when the hand position is not modified, and those in the second row do when it is modified. It is observed that the small

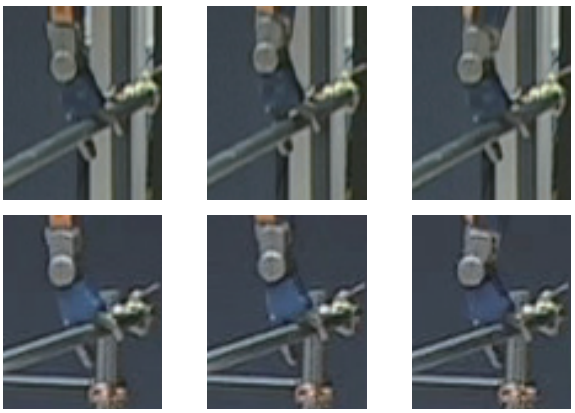

Fig. 9. Effect of the hand position control

room between the hand and the handrail is removed after the modification.

C. Continuous walking using the waist joints

As described above, the robot has to stop after stepping over a box, since the reachable range of the hand is too limited to support the body continuously. The constraint can be relaxed when the waist joints of the robot are used. To this end, $\dot{\boldsymbol{\theta}}_{arm_i}$ is replaced by $\dot{\boldsymbol{\theta}}_{upper_i} = [\dot{\boldsymbol{\theta}}^T_{waist}, \dot{\boldsymbol{\theta}}^T_{arm_i}]^T$ and $\boldsymbol{J}_{arm}$ by $\boldsymbol{J}_{upper_i} = [\boldsymbol{J}_{waist}\ \boldsymbol{J}_{arm_i}]$, then Eq.(4) becomes

$$\dot{\boldsymbol{\theta}}_{upper_i} = \boldsymbol{J}^{\dagger}_{upper_i} \left(\begin{bmatrix} \boldsymbol{v}_{H_i} \\ \boldsymbol{\omega}_{H_i} \end{bmatrix} - \begin{bmatrix} \boldsymbol{E} & -\hat{\boldsymbol{r}}_{B\to H_i} \\ \boldsymbol{0} & \boldsymbol{E} \end{bmatrix} \begin{bmatrix} \boldsymbol{v}_B \\ \boldsymbol{\omega}_B \end{bmatrix} \right) + (\boldsymbol{E} - \boldsymbol{J}^{\dagger}_{upper_i} \boldsymbol{J}_{upper_i}) \boldsymbol{K} (\boldsymbol{\theta}^{ref}_{upper_i} - \boldsymbol{\theta}_{upper_i}),$$

where $()^{\dagger}$ is the pseudo inverse of a matrix, $\boldsymbol{K}$ a gain matrix, and $\boldsymbol{\theta}^{ref}_{upper_i}$ desired angles of $\boldsymbol{\theta}_{upper_i x}$ which are give to make the waist joints rotate more and let the arm joints stay in the feasible ranges. Note that the waist joints are determined by solving the inverse kinematics for the arm whose hand touches the handrail and that the obtained joint angles are used when the inverse kinematics of another arm is solved. The equations of the momentum are modified into

$$\begin{bmatrix} \mathcal{P} \\ \mathcal{L} \end{bmatrix} = \begin{bmatrix} \boldsymbol{M}^*_B \\ \boldsymbol{H}^*_B \end{bmatrix} \boldsymbol{\xi}_B + \sum_{i=1}^{2} \left\{ \begin{bmatrix} \boldsymbol{M}^*_{F_i} \\ \boldsymbol{H}^*_{F_i} \end{bmatrix} \boldsymbol{\xi}_{F_i} + \begin{bmatrix} \boldsymbol{M}^*_{H_i} \\ \boldsymbol{H}^*_{H_i} \end{bmatrix} \boldsymbol{\xi}_{H_i} \right\} + \sum_{i=1}^{2} \begin{bmatrix} \boldsymbol{M}_{upper_i} \\ \boldsymbol{H}_{upper_i} \end{bmatrix} (\boldsymbol{E} - \boldsymbol{J}^{\dagger}_{upper_i} \boldsymbol{J}_{upper_i}) \phi,$$

where

$$\begin{aligned} \begin{bmatrix} \boldsymbol{M}^*_B \\ \boldsymbol{H}^*_B \end{bmatrix} &\equiv \begin{bmatrix} M\boldsymbol{E} & -M\hat{\boldsymbol{r}}_{B\to G} \\ \boldsymbol{0} & \tilde{\boldsymbol{I}} \end{bmatrix} - \sum_{i=1}^{2} \begin{bmatrix} \boldsymbol{M}^*_{F_i} \\ \boldsymbol{H}^*_{F_i} \end{bmatrix} \begin{bmatrix} \boldsymbol{E} & -\hat{\boldsymbol{r}}_{B\to F_i} \\ \boldsymbol{0} & \boldsymbol{E} \end{bmatrix} - \sum_{i=1}^{2} \begin{bmatrix} \boldsymbol{M}^*_{H_i} \\ \boldsymbol{H}^*_{H_i} \end{bmatrix} \begin{bmatrix} \boldsymbol{E} & -\hat{\boldsymbol{r}}_{B\to H_i} \\ \boldsymbol{0} & \boldsymbol{E} \end{bmatrix}, \\ \begin{bmatrix} \boldsymbol{M}^*_{F_i} \\ \boldsymbol{H}^*_{F_i} \end{bmatrix} &\equiv \begin{bmatrix} \boldsymbol{M}_{leg_i} \\ \boldsymbol{H}_{leg_i} \end{bmatrix} \boldsymbol{J}^{-1}_{leg_i}, \\ \begin{bmatrix} \boldsymbol{M}^*_{H_i} \\ \boldsymbol{H}^*_{H_i} \end{bmatrix} &\equiv \begin{bmatrix} \boldsymbol{M}_{upper_i} \\ \boldsymbol{H}_{upper_i} \end{bmatrix} \boldsymbol{J}^{\dagger}_{upper_i}, \\ \phi &= \boldsymbol{K}(\boldsymbol{\theta}^{ref}_{upper_i} - \boldsymbol{\theta}_{upper_i}). \end{aligned}$$

The walking in Fig.5 was made continuous without the halt by using the waist joints, and Fig.10 shows pictures of the intermedicate motions using the waist joints in the simulation and the experiment. The forces to the right hand

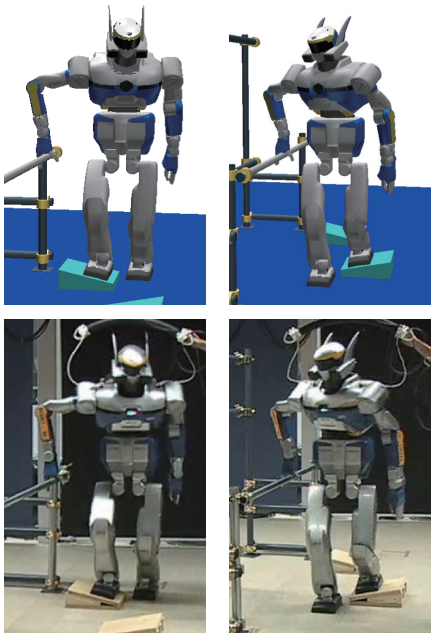

Fig. 10. Walking using the waist joints

during the continuous walking in the simulation (left) and

the experiment (right) are shown in Fig.11 respectively, and the trajectories of the CWS on $\tau_x\tau_y$-plane in Fig.12. When

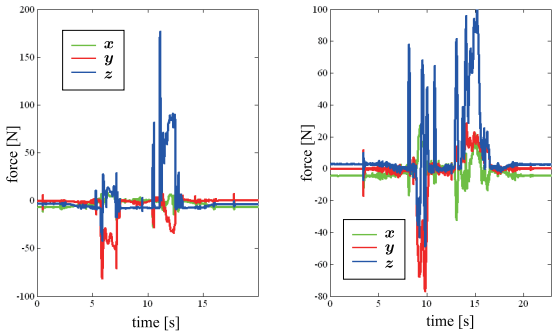

Fig. 11. Force to the hand in the simulation and the experiment

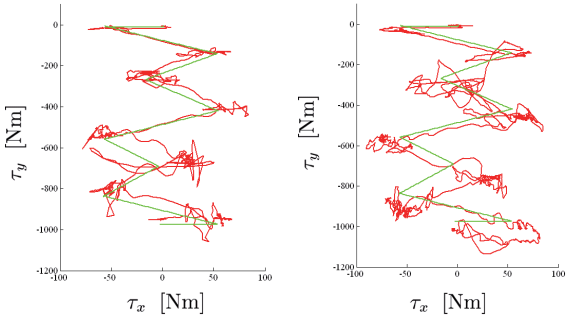

Fig. 12. Trajectories of the CWS in the simulation and the experiment

the hand touches to the handrail at the second contact point, the reference of the CWS is specified to let the hand have a positive vertical force which can be clearly observed in the graph of the experiment. The trajectoriy of the CWS follows the reference in a practical degree.

IV. CONCLUSIONS

The contributions of the paper can be summarized as follows.

- A pattern generator of a humanoid robot that walks on a rough terrain while touching a handrail was proposed. It is guaranteed rigorously that the generated pattern should keep the desired contact between the robot and the environment consisting of the handrail and the terrain under the sufficient friction assumption.
- The pattern generator was successfully applied to a biped humanoid robot that walks on tilted steps with a support of a handrail.
- It was confirmed that the hand position control is able to improve the stability of the contact.
- The generator was enhanced to use the waist joints for extending the reachable range of a hand that has contributed to realize the continuous walking.

It is assumed that the position and the geometry of the handrail and the terrain are known *a prior*. Future works include the introduction of sensing of the working environment and a feedback control to cope with possible errors of the sensing.

ACKNOWLEDGMENTS

This study was performed as one of the Coordination Program of Science and Technology Projects “Next Generation Robots”, conducted by the Council of Science and Technology Policy (CSTP) and funded by Special Coordination Fund for Promoting Science and Technology.

REFERENCES

[1] A.Goswami, Postural stability of biped robots and the foot rotation indicator (FRI) point, Int. J. Robotics Research, vol.19, no.6, pp.523-533, 1999.
[2] K.Harada, S.Kajita, K.Kaneko, and H.Hirukawa, ZMP Analysis for Arm/Leg Coordination, Proc. IEEE/RSJ Int. Conf. on Intelligent Robots and Systems, Oct.2003.
[3] K.Harada, H.Hirukawa, F.Kanehiro, K.Fujiwara, K.Kaneko, S.Kajita and M.Nakamura, Dynamic Balance of a Humanoid Robot grasping an Environment, Proc. IEEE/RSJ Int. Conf. on Intelligent Robots and Systems, Oct.2004.
[4] H.Hirukawa, S.Hattori, K.Harada, S.Kajita, K.Kaneko, F.Kanehiro, K.Fujiwara and M.Morisawa, A Universal Stability Criterion of the Foot Contact of Legged Robots – Adios ZMP, Prof. IEEE Int. Conf. on Robotics and Automation, 2006.
[5] H.Hirukawa, S.Hattori, S.Kajita, K.Harada, K.Kaneko, F.Kanehiro, M.Morisawa and S.Nakaoka, A Pattern Generator of Humanoid Robots walking on a Rough Terrain, Proc. IEEE Int. Conf. on Robotics and Automation, 2007.
[6] S.Kajita, F. Kanehiro, K. Kaneko, K. Fujiwara, K. Harada, K. Yokoi, H. Hirukawa, Biped Walking Pattern Generation by using Preview Control of Zero-Moment Point, Proc. IEEE Int. Conf. on Robotics and Automation, 2003.
[7] S.Kajita, F.Kanehiro, K.Kaneko, K.Fujiwara, K.Harada, K.Yokoi and H.Hirukawa, Resolved Momentum Control: Humanoid Motion Planning based on the Linear and Angular Momentum, Prof. IEEE Int. Conf. on Intelligent Robots and Systems, 2003.
[8] F.Kanehiro, H.Hirukawa and S.Kajita, OpenHRP: Open Architecture Humanoid Robotics Platform, International Journal of Robotics Research, vol.23, no.2, pp.155–165, 2004.
[9] K.Kaneko, F.Kanehiro, S.Kajita, H.Hirukawa, T.Kawasaki, M.Hirata, K.Akachi and T.Isozumi, Humanoid Robot HRP-2, Prof. IEEE Int. Conf. on Robotics and Automation, 2004.
[10] S.Nakaoka, S.Hattori, F.Kanehiro, S.Kajita and H.Hirukawa, Constraint-based Dynamics Simulator for Humanoid Robots with Shock Absorbing Mechanisms, IEEE/RSJ Int. Conf. on Intelligent Robots and Systems, 2007.
[11] K.Nishiwaki, S.Kagami, Y.Kuniyoshi, M.Inaba and H.Inoue, Online Generation of Humanoid Walking Motion based on a Fast Generation Method of Motion Pattern that Follows Desired ZMP, Prof. IEEE Int. Conf. on Intelligent Robots and Systems, 2002.
[12] H.O.Lim, Y.Kaneshima, A.Takanishi, Online Walking Pattern Generation for Biped Humanoid Robot with Trunk, Prof. IEEE International Conference on Robotics and Automation, vol.3, pp.3111-3116, 2002.
[13] J.Pang and J.Trinkle, Stability characterizations of rigid body contact problems with Coulomb friction, Zeitschrift fur Angewandte Mathematik und Mechanik, vol.80, no.10, pp.643-663, 2000.
[14] T.Saida, Y.Yokokoji and T.Yoshikawa, FSW (feasible solution of wrench) for Multi-legged Robots, Proc. IEEE Int. Conf. on Robotics and Automation, pp.3815-3820, 2003.
[15] M.Vukobratovic and J.Stepanenko, On the stability of Anthropomorphic Systems, Mathematical Biosciences, vol.15, pp.1-37, 1972.
[16] K.Yamane and Y.Nakamura, Parallel O(logN) Algorithm for Dynamics Simulation of Humanoid Robots, IEEE-RAS Int. Conf. on Humanoid Robots, pp.554-559, 2006.
[17] K.Yoneda and S.Hirose, Tumble Stability Criterion of Integrated Locomotion and Manipulation, Proc. IEEE/RSJ Int. Conf. on Intelligent Robots and Systems, pp.870-876, 1996.